



# Host (nanocavity of zeolite-Y or X)–guest (manganese (III) *tetrakis*[4-*N*-methylpyridinium]porphyrin) nanocomposite materials as efficient catalysts for biomimetic alkene epoxidation with sodium periodate: Shape-selective epoxidation of linear alkenes

Majid Moghadam\*, Shahram Tangestaninejad\*, Valiollah Mirkhani, Iraj Mohammadpoor-Baltork, Maryam Moosavifar

Department of Chemistry, Catalysis Division, University of Isfahan, Isfahan 81746-7344, Iran

## ARTICLE INFO

### Article history:

Received 19 June 2008

Received in revised form

25 November 2008

Accepted 30 November 2008

Available online 6 December 2008

### Keywords:

Biomimetic catalysts

Epoxidation

Sodium periodate

Zeolite

Manganese porphyrin

## ABSTRACT

Manganese (III) 5,10,15,20-*tetrakis*(4-*N*-methylpyridyl) porphyrin encapsulated into zeolite X, [Mn(TMPyP)-NaX], and zeolite Y, [Mn(TMPyP)-NaY] was synthesized through the zeolite synthesis method, in which NaX and NaY zeolites were synthesized around one cationic Mn porphyrin. The syntheses yielded pure MnP-NaX and MnP-NaY catalysts without any by-products blocking the zeolite nanopores. These heterogenized catalysts were characterized by FT-IR, UV-vis spectroscopic techniques, X-ray diffraction (XRD), neutron activation analysis (NAA) and thermal analysis. These catalysts were used for efficient and selective alkene epoxidation with NaIO<sub>4</sub> under mechanical stirring and under ultrasonic irradiation. These catalysts were also used for epoxidation of linear alkenes and good shape selectivity was observed.

© 2008 Elsevier B.V. All rights reserved.

## 1. Introduction

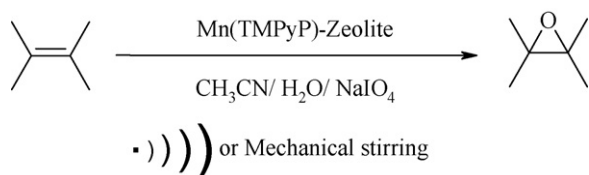
In biomimetic systems, synthetic metalloporphyrins (MeP) have been used as attractive building blocks for the molecular engineering with designed chemical, physical, or catalytic properties [1]. The selectivity and stability in the biomimetic oxidation systems are originated from steric and electronic effects [2–6]. This is why there is a growing interest on mimicking the protein cavity of natural enzymes. Immobilization of metalloporphyrins to solid matrixes such as silica [7–9] and chemically modified silica surfaces [10,11], zeolites [12] or organic polymers [13–16] have been carried out in order to obtain more efficient oxidation systems and mimic the action of heme enzymes such as peroxidases [17,18] and cytochrome P-450 [19–22].

Zeolites can be used as enzymatic model due to the molecular-size channels and pores in three-dimensional network of well-defined crystalline structures which confers shape and size selectivity [23]. Zeolite-encapsulated metalloporphyrins, MP,

present many advantages such as replacement of zeolite as the protein portion of natural enzymes and proving a controlled steric environment for the MeP, serving as a model for the active site of cytochrome P-450 [24–26]. These systems show the chemoselectivity, regioselectivity and stereoselectivity in model reactions [27].

Cationic porphyrins have extensively studied as templates in the synthesis of molecular sieves such as aluminosilicates, aluminophosphates and gallophosphates [6]. Due to their stability under hydrothermal synthetic conditions and their solubility, these metalloporphyrins are used extensively in the method of “build-bottle-around-ship” [12,28,29]. This model is considered as a complete mimic enzymatic of the inorganic matrix that the activation of substrate occurred by porphyrin catalytic centre [30,31]. So, with forming metallocomplexes into zeolite cages, the complex may have a unique configuration, which may differ from that form existing in solution [32–34]. In this way, cationic metalloporphyrins are stabilized inside the negative framework of the zeolite cavities through an electrostatic interaction [33]. Furthermore, heterogeneous metalloporphyrins have advantages such as steric and electronic effects of the support that are similar to the influence of the polypeptide chain in hemoproteins and provide an easy way to recover and recycle them from the reaction media [12,35–37].

\* Corresponding authors. Tel.: +98 311 7932705; fax: +98 311 6689732.  
E-mail addresses: [moghadamm@chem.ui.ac.ir](mailto:moghadamm@chem.ui.ac.ir), [moghadamm@sci.ui.ac.ir](mailto:moghadamm@sci.ui.ac.ir), [majidmoghadamz@yahoo.com](mailto:majidmoghadamz@yahoo.com) (M. Moghadam), [stanges@sci.ui.ac.ir](mailto:stanges@sci.ui.ac.ir) (S. Tangestaninejad).



**Scheme 1.** Oxidation of alkenes with  $\text{NaO}_4$  catalyzed by  $\text{Mn(TMPyP)}$ -zeolites.

Battioni et al. have described the catalytic activity of some metalloporphyrins encapsulated in  $\text{NH}_4\text{-Y}$  zeolite, where the porphyrin complexes have synthesized inside the Y zeolite, by template synthesis method [38]. Balkus et al. have used the zeolite synthesis method to synthesize zeolite NaX around cobalt (II) and copper (II) phthalocyanine complexes [39]. Rosa et al. have used zeolite synthesis method in which the anionic framework of NaX zeolite is synthesized around the cationic iron (III) porphyrins and applied these catalysts in the oxidation of hydrocarbons [12]. Zhan and Li have reported the synthesis of a faujasite Y confined metalloporphyrin, and investigated its catalytic activity in the oxidation of cyclohexene [28].

In this paper, we describe the preparation, physicochemical characterization and application of two NaX and NaY zeolites-encapsulated  $\text{Mn(III)}$ -porphyrin in the epoxidation of cyclic, linear and branched alkenes with  $\text{NaO}_4$  under mechanical stirring and ultrasonic irradiation conditions (Scheme 1).

## 2. Experimental

All solvents and reagents were of commercial grade and obtained from Merck and Fluka. Alkenes were passed through a column containing active alumina to remove the peroxidic impurities.

### 2.1. Preparation of zeolite-encapsulated $\text{MnP-NaX}$

Porphyrin ligand was purchased from Fluka and was used without prior purification. The manganese porphyrin was prepared according to the literature [11]. The manganese (III) tetrapyrrolylporphyrin was methylated by reaction with large excess (360 equiv.) of  $\text{CH}_3\text{I}$  at room temperature under argon atmosphere [25].

The  $\text{MnP-NaX}$  catalysts were synthesized through the method reported by Balkus et al. [39]. A silicate gel was prepared by stirring of silica (3.5 g),  $\text{NaOH}$  (3 g) and the desired  $\text{MnP}$  ( $1.8 \times 10^{-4}$  mol) in  $\text{H}_2\text{O}$  (7.5 ml). The gel was then added to an aluminate solution containing aluminum isopropoxide ( $\text{Al}[\text{OCH}(\text{CH}_3)_2]_3$ ) (7.75 g),  $\text{NaOH}$  (3.25 g) and  $\text{H}_2\text{O}$  (10 ml). This mixture was transferred to a polypropylene bottle containing  $\text{H}_2\text{O}$  (30 ml) and stirred at room temperature for 24 h. The crystallization occurred at  $90^\circ\text{C}$  under static and autogeneous conditions in a stainless steel bomb (100 ml) for 15 h. Then  $\text{H}_2\text{O}$  (20 ml) was added and the resulting solids were filtered, washed several times with water and dried at  $80^\circ\text{C}$  for 24 h. The complexes adsorbed on the external surface of the zeolite were removed through Soxhlet extraction with water, and then with methanol to remove all the  $\text{MnP}$  present on the external surface of the zeolite. The samples were dried at  $80^\circ\text{C}$  for 24 h.

### 2.2. Preparation of zeolite-encapsulated $\text{MnP-NaY}$

The  $\text{MnP-NaY}$  catalyst was synthesized according to the procedure for the inclusion of cationic metalloporphyrins inside the nanocages of faujasites X and Y during hydrothermal synthesis [12]. The aluminosilicate gel was prepared by stirring of colloidal silica (4.6 g), sodium hydroxide (6.2 g), sodium aluminate (3.2 g) and  $\text{H}_2\text{O}$  (80 ml). After then,  $\text{MnP}$  (0.42 g,  $3.6 \times 10^{-4}$  mol) was added.

The crystallization occurred at  $95^\circ\text{C}$  under static and autogeneous conditions in a stainless steel bomb (250 ml) for 48 h. The complexes adsorbed on the external surface of the zeolite were removed through Soxhlet extractions with distilled water, methanol. The final product was dried at  $60^\circ\text{C}$  for 24 h.

### 2.3. Instrumentation

The electronic spectra of the ligand and complex in the UV-vis region were recorded in methanol solution using a Shimadzu 160 UV-vis or a Varian Cary NIR spectrophotometer. Powder X-ray diffraction of the hybrid compounds were carried out with  $\text{Cu K}\alpha$  radiation and a graphite monochromatic with scan speed  $16^\circ/\text{min}$ . Gas chromatography (GC) experiments performed with a Shimadzu GC-16A instrument using a 2 m column peaked with silicon DC-200 or Carbowax 20m using *n*-decane as internal standard. FT-IR spectra were obtained as potassium bromide pellets in the range  $400\text{--}4000\text{ cm}^{-1}$  with a Nicolet-Impact 400D instrument. Atomic absorption spectra (AAS) were recorded on a Perkin-Elmer 3110 Spectrophotometer using a flame approach. Diffuse reflectance spectra were recorded on a Shimadzu UV-265 instrument using optical grade  $\text{BaSO}_4$  as reference.

### 2.4. General procedure for oxidation reactions catalyzed by $\text{MnP-NaX}$ or $\text{MnP-NaY}$ under mechanical stirring

All of the reactions were carried out at room temperature under air in a 25-ml flask equipped with a magnetic stirrer bar. To a mixture of alkene (0.5 mmol), imidazole (1.4 mmol), manganese porphyrin ( $7\ \mu\text{mol}$  for  $\text{MnP-NaX}$  and  $16\ \mu\text{mol}$  for  $\text{MnP-NaY}$ ) and  $\text{CH}_3\text{CN}$  (5 ml) was added a solution of  $\text{NaO}_4$  (1 mmol) in  $\text{H}_2\text{O}$  (2.5 ml). The progress of reaction was monitored by GC. The reaction mixture was diluted with  $\text{Et}_2\text{O}$  (20 ml) and filtered. The catalyst was thoroughly washed with  $\text{Et}_2\text{O}$  and combined washings and filtrates were purified on a silica-gel plates or a silica-gel column. IR and  $^1\text{H}$  NMR spectral data confirmed the identities of the products.

### 2.5. General procedure for oxidation reactions catalyzed by $\text{MnP-NaX}$ or $\text{MnP-NaY}$ under ultrasonic irradiation

All reactions were carried out at room temperature in a 40-ml glass reactor. A UP 400S ultrasonic processor equipped with a 3-mm wide and 140-mm long probe, which was immersed directly into the reaction mixture, was used for sonication. The operating frequency was 24 kHz and the output power was set at 0–400 W through manual adjustment. The total volume of the solution was 15 ml. The temperature reached to  $40^\circ\text{C}$  during sonication.

A solution of  $\text{NaO}_4$  (2 mmol in 5 ml  $\text{H}_2\text{O}$ ) was added to a mixture of alkene (1 mmol) and imidazole (2.8 mmol) in  $\text{CH}_3\text{CN}$  (10 ml). After addition of manganese porphyrins ( $7\ \mu\text{mol}$  for  $\text{MnP-NaX}$  and  $16\ \mu\text{mol}$  for  $\text{MnP-NaY}$ ), the mixture was sonicated. Progress of the reaction was followed by GC. At the end of reaction, the catalyst was filtered off and the filtrates were extracted with  $\text{Et}_2\text{O}$  and were purified on a silica-gel plate or a silica-gel column (eluent:  $\text{CCl}_4\text{-Et}_2\text{O}$ ). The identities of products were confirmed by IR and  $^1\text{H}$  NMR spectral data.

## 3. Results and discussion

### 3.1. Preparation and characterization of zeolite NaY- and NaX-encapsulated $\text{Mn(III)}$ -porphyrin

The synthesis of zeolite Y-encapsulated  $\text{Mn(III)}$ -porphyrin,  $\text{MnP-NaY}$ , and zeolite X-encapsulated  $\text{Mn(III)}$ -porphyrin,  $\text{MnP-NaX}$ , was carried out by a zeolite synthesis method [38,40]. In these methods, the anionic host was synthesized around the cationic

guest through an electrostatic interaction. Therefore, no free metal ion, free ligand or impurities like polypyrrins (which result from metalloporphyrin synthesis) [12] in the zeolite cages are present, and as a result, no complication in characterization (presence of a broad band at  $\sim 480$  nm) and reactivity (pore blockage) of the resulting material are observed [41].

Upon formation of metalloporphyrin cations into zeolite cages, the originally white zeolites turn to brown (bright brown in Mn(TMPyP)-NaX and dark brown in Mn(TMPyP)-NaY). The color of obtained material after the washings with Soxhlet extraction remained constant which indicated the incorporation of metalloporphyrins into NaX and NaY zeolites. This difference in the color of two encapsulated metalloporphyrins is due to the amount of metalloporphyrin loading into the zeolites. Therefore, this factor affects the reactivity and selectivity of two encapsulated metalloporphyrins in the epoxidation of alkenes. The UV-vis spectra of both MnP-NaX and MnP-NaY after digestion of them in acid showed similar spectra of free MnP complex in solution (Table 1). No significant change was observed in the position of the Q and Soret bands in comparison with the values observed for respective metalloporphyrins in solutions. This confirms the incorporation of metalloporphyrin into zeolites without any spatial confinement and the metalloporphyrin has been dispersed into the nanocages of zeolites. The size of nanocages of zeolites is 1.3 nm and the size of metalloporphyrin is 1.2 nm [34], then it is expected that insertion of metalloporphyrin occurs without spatial strain.

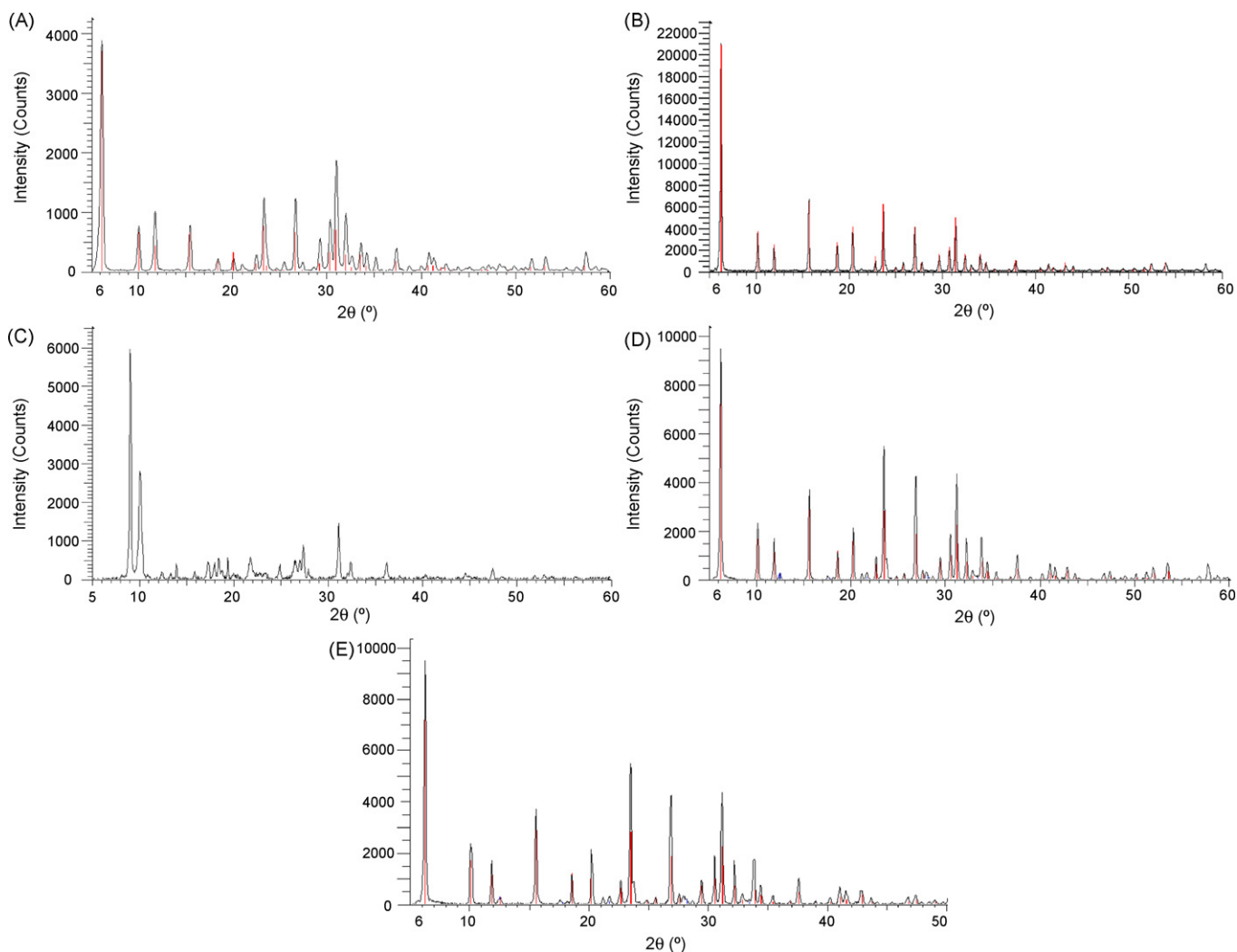
**Table 1**

Amount of metalloporphyrin retained by the zeolite X and zeolite Y and UV-vis absorption bands for Mn(TMPyP).

Entry	Catalyst	Metalloporphyrin loading (mmol/100 g zeolite)	Wavelength (nm)		
			CT-band	Soret band	Q-band
1	Mn (TMPyP)	–	398 (376)	462	558
2	Mn (TMPyP)-NaX	0.69	397	461	557
3	Mn (TMPyP)-NaY	1.35	397 (377)	462	558

Comparison of UV-vis spectrum of Mn(TMPyP) complex and the diffuse reflectance spectra of Mn(TMPyP) encapsulated in zeolites Y and X (Fig. 1), confirmed the incorporation of metalloporphyrin into the supercages of zeolites. The same band is present in the UV-vis spectra of Mn(TMPyP) entrapped in the NaY and NaX zeolites but the maxima have been shifted to lower wavelength. Such blue shift of the absorption band in comparison with the free metalloporphyrin indicates that the immobilization of the complex modifies the electronic and spectral properties of the encapsulated metalloporphyrin.

The XRD patterns indicated that the NaY and NaX zeolites-encapsulated metallocomplexes have crystallinity almost identical to that of the parent NaY and NaX zeolites (Fig. 2). It is apparent that encapsulation conditions have little impact on the



**Fig. 1.** XRD patterns of: (A) NaX zeolite, (B) NaX zeolite, (C) MnP, (D) MnP-NaY, and (E) MnP-NaX.

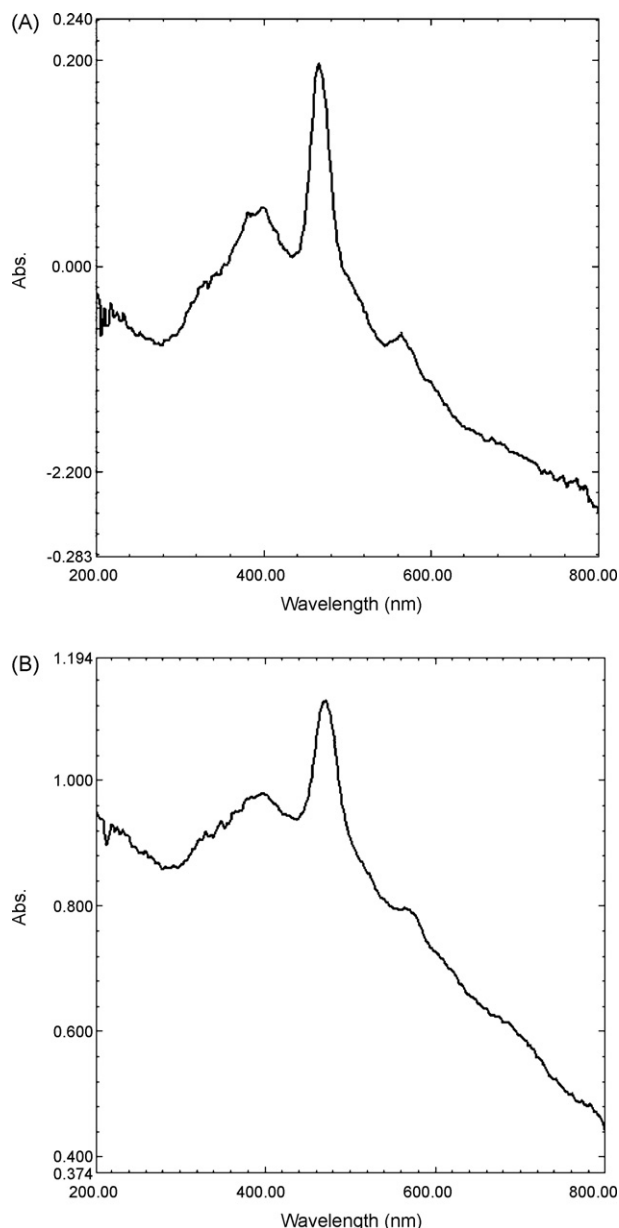


Fig. 2. Diffuse reflectance spectra of: (A) MnP-NaY and (B) MnP-NaX.

crystallinity of the zeolites host. This fact can be due to their fine distribution in the lattice [27,42].

FT-IR spectra for NaX and NaY zeolites show strong zeolite lattice bands in the range  $450\text{--}1200\text{ cm}^{-1}$ . The strong band at the  $1032\text{ cm}^{-1}$  could be attributed to the asymmetric stretching vibrations of  $(\text{Si}/\text{Al})\text{O}_4$  units [43]. The broad band at the  $1637$  and  $3465\text{ cm}^{-1}$  are due to lattice water molecules and surface hydroxyl groups. The FT-IR spectra of NaY zeolite and encapsulated metalloporphyrins are presented in Fig. 3. No shift was observed in the zeolite lattice bands of encapsulated metalloporphyrins, which further implies that the zeolite framework has retained unchanged upon the encapsulation of metalloporphyrin. The bands observed in the  $1200\text{--}1600\text{ cm}^{-1}$ , where zeolite has no bands, confirmed the presence of metalloporphyrin in the zeolite pores. However, due to low concentration of metalloporphyrin in the NaX and NaY zeolites, the metalloporphyrin bands have weak intensity. However, it is possible to observe bands at  $1150\text{--}1550$  and  $2800\text{--}3200\text{ cm}^{-1}$  attributed to C–C and C=N vibrations of the porphyrin ring and C–H vibrations for the Mn(TMPyP)-NaX, respectively [44–46].

Table 2

The effect of solvent on the epoxidation of cyclooctene with  $\text{NaIO}_4$  catalyzed by MnP-NaX at room temperature<sup>a</sup>.

Solvent	Epoxide yield (%) after 10 h <sup>b</sup>
$\text{CH}_3\text{CN}/\text{H}_2\text{O}$	94
$\text{CH}_3\text{COCH}_3/\text{H}_2\text{O}$	45
$\text{CH}_3\text{OH}/\text{H}_2\text{O}$	28.5
$\text{CH}_2\text{Cl}_2/\text{H}_2\text{O}$	2

<sup>a</sup> Cyclooctene (0.5 mmol),  $\text{NaIO}_4$  (1 mmol), catalyst (MnP-NaX, 0.007 mmol), solvent (5 ml),  $\text{H}_2\text{O}$  (2.5 ml).

<sup>b</sup> GC yield.

Table 3

The effect of axial ligand on the epoxidation of cyclooctene with  $\text{NaIO}_4$  catalyzed by MnP-NaX at room temperature<sup>a</sup>.

Axial ligand	Epoxide yield (%) after 5 h <sup>b</sup>
Imidazole	94
1-Methyl pyridine	20
Pyridine	40
2-Methyl pyridine	30
No axial ligand	2
No catalyst	0

<sup>a</sup> Cyclooctene (0.5 mmol),  $\text{NaIO}_4$  (1 mmol), catalyst (0.007 mmol),  $\text{CH}_3\text{CN}$  (5 ml),  $\text{H}_2\text{O}$  (2.5 ml).

<sup>b</sup> GC yield.

The amounts of manganese porphyrin on the supported catalysts were determined by atomic absorption spectroscopy and neutron activation analysis, which showed value of  $0.0135\text{ mmol/g}$  for Mn(TMPyP)-NaY and  $0.0069\text{ mmol/g}$  for Mn(TMPyP)-NaX.

One possible explanation for higher metalloporphyrin loading for NaX zeolite is related to difference in Si/Al ratio in NaX and NaY zeolites. The Si/Al ratio is 1.5–3 for NaY and 1–1.5 for NaX zeolites. When the Al content of zeolite becomes more, the capacity of cations exchange is enhanced and therefore, the number of sites which is occupied by cations increases [47]. In the case of NaX zeolite, only a few metal complexes are inserted into supercage of zeolite and the content of encapsulated metallo complexes is lower than NaY zeolite.

### 3.2. Effect of solvent on the oxidation of cyclooctene

Solvent plays an important role in catalytic behavior of epoxidation catalysts because it can uniform the different phases and therefore, promoting mass transportation, and can also change the reaction mechanism by affecting the intermediate species, the surface properties of catalysts and reaction pathways [48]. Among the mixture of methanol, ethanol, acetone, acetonitrile, and dichloromethane with water, the 2:1 mixture of acetonitrile/water was chosen as the reaction medium, because the higher epoxidation yield was observed. The results are shown in Table 2.

### 3.3. Effect of axial ligand on the epoxidation of cyclooctene

The effect of different axial ligands on the catalytic activity of MnP-NaX and MnP-NaY in the epoxidation of cyclooctene was studied. The best results were obtained in the presence of imidazole (Table 3). When the same reaction was carried out in the absence of imidazole, only small amounts of cyclooctene oxide was detected in the reaction mixture.

### 3.4. Catalytic alkene epoxidation with $\text{NaIO}_4$ in the presence of Mn(TMPyP)-NaX and Mn(TMPyP)-NaY under mechanical stirring

The epoxidation of alkenes with  $\text{NaIO}_4$  in presence of Mn(TMPyP)-NaX and Mn(TMPyP)-NaY yielded the corresponding

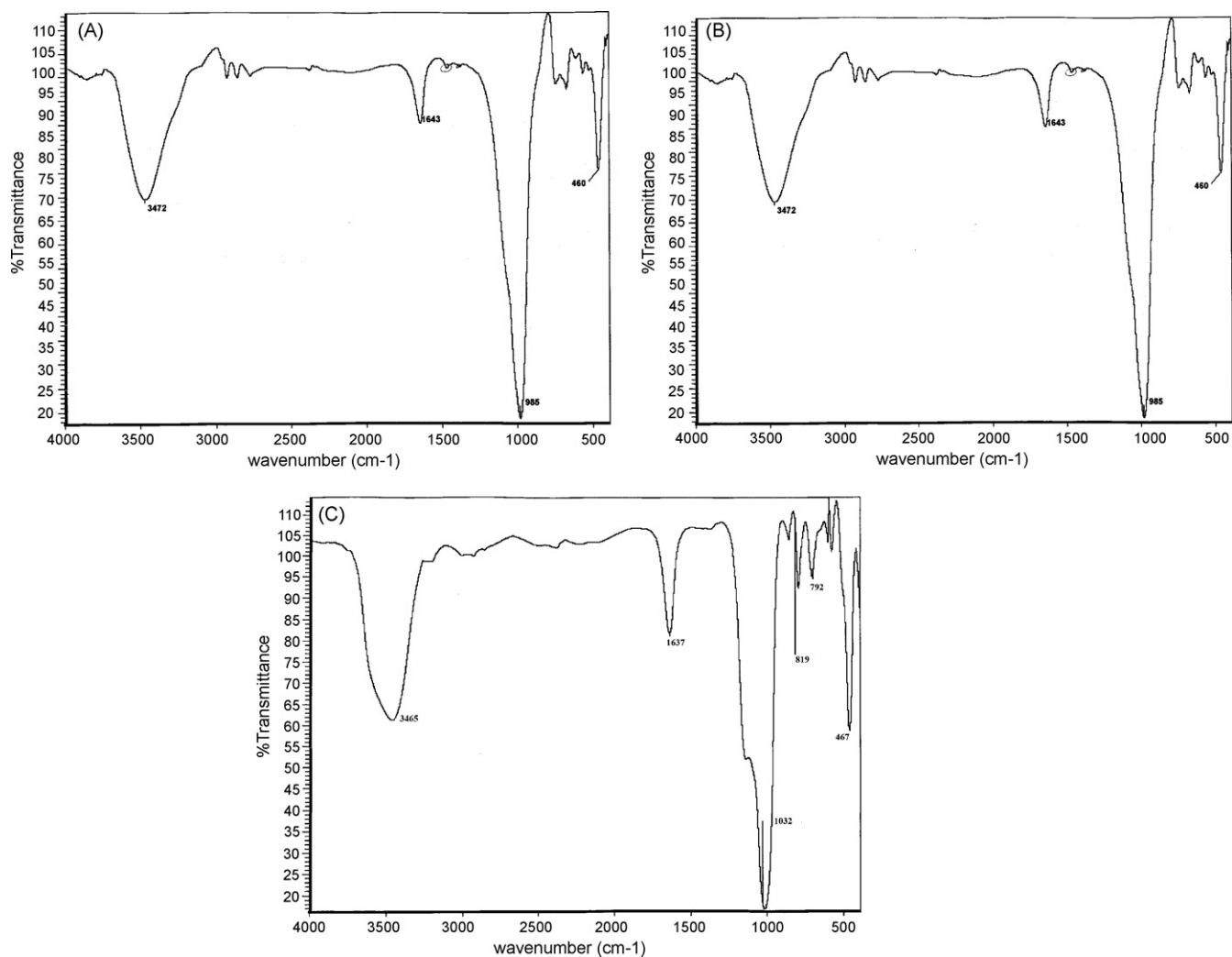


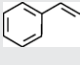
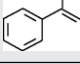


Fig. 3. FT-IR spectra of: (A) MnP-NaY, (B) MnP-NaX, and (C) MnP.

oxide products in aqueous acetonitrile at room temperature (Table 4). Cyclooctene was converted to cyclooctene oxide in two catalytic systems in high yield. Epoxidation of styrene with the former system produced 16% benzaldehyde and 67% styrene oxide, whereas in the later system 30% benzaldehyde and 70%

styrene oxide was produced. In the epoxidation of cyclohexene with Mn(TMPyP)-NaX/NaIO<sub>4</sub> catalytic system, the yield of epoxide was 68% and with Mn(TMPyP)-NaY/NaIO<sub>4</sub> system was 53%. While in both systems, the allylic oxidation was also observed.

**Table 4**  
Epoxidation of alkenes with NaIO<sub>4</sub> catalyzed by MnP-NaX and MnP-NaY under mechanical stirring<sup>a</sup>.

Entry	Alkene	MnP-NaX				MnP-NaY			
		Conversion (%) <sup>b</sup>	Epoxide selectivity (%)	Time (h)	TOF (h <sup>-1</sup> )	Conversion (%) <sup>b</sup>	Epoxide selectivity (%)	Time (h)	TOF (h <sup>-1</sup> )
1		95	100	5.5	22.05	97	100	5	11.98
2		97 <sup>c</sup>	76	8	14.59	100 <sup>c</sup>	53	6.5	9.10
3		83 <sup>d</sup>	79	11	8.09	100 <sup>d</sup>	70	10	10.26
4		97	100	10	21.43	100	100	8	20.17

<sup>a</sup> Reaction conditions: alkene (0.5 mmol), NaIO<sub>4</sub> (1 mmol), catalyst (600 mg), CH<sub>3</sub>CN/H<sub>2</sub>O (5/2.5 ml).

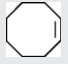

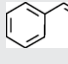
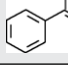
<sup>b</sup> GC yield.

<sup>c</sup> The by-products are 8% allylic alcohol and 18% allylic ketone for MnP-NaX and 19% allylic alcohol and 28% allylic ketone for MnP-NaY.


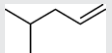





<sup>d</sup> Benzaldehyde was produced as by-product.



**Table 5**  
Epoxidation of alkenes with NaIO<sub>4</sub> catalyzed by MnP-NaX and MnP-NaY under ultrasonic irradiation<sup>a</sup>.

Entry	Alkene	MnP-NaX				MnP-NaY			
		Conversion (%) <sup>b</sup>	Epoxide selectivity (%)	Time (min)	TOF (h <sup>-1</sup> )	Conversion (%) <sup>b</sup>	Epoxide selectivity (%)	Time (min)	TOF (h <sup>-1</sup> )
1		100	100	35	213.85	98	100	20	177.85
2		100 <sup>c</sup>	68	30	242.93	100 <sup>c</sup>	63	30	121.98
3		95 <sup>d</sup>	80	120	56.57	100 <sup>d</sup>	89	50	74.07
4		95 <sup>e</sup>	60	60	108.2	96	55 <sup>e</sup>	20	157.50

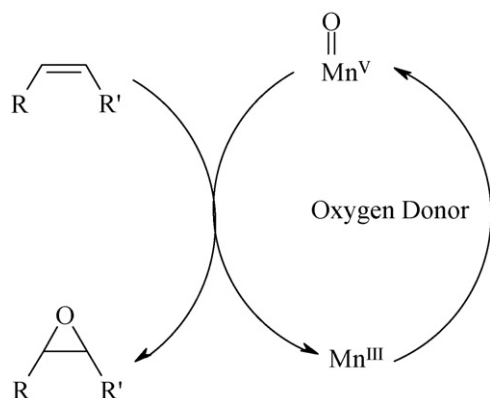
<sup>a</sup> Reaction conditions: alkene (0.5 mmol), NaIO<sub>4</sub> (1 mmol), catalyst (600 mg), CH<sub>3</sub>CN/H<sub>2</sub>O (5/2.5 ml).<sup>b</sup> GC yield.<sup>c</sup> The by-products are 17% allylic alcohol and 15% allylic ketone for MnP-NaX and 15% allylic alcohol and 22% allylic ketone for MnP-NaY.<sup>d</sup> Benzaldehyde was produced as by-product.<sup>e</sup> Acetophenone was produced as by-product.**Table 6**  
Epoxidation of linear alkenes with NaIO<sub>4</sub> catalyzed by MnP-NaX and MnP-NaY under mechanical stirring<sup>a</sup>.

Entry	Alkene	MnP-NaX			MnP-NaY		
		Conversion (%) <sup>b</sup>	Epoxide selectivity (%)	Time (h)	Conversion (%) <sup>b</sup>	Epoxide selectivity (%)	Time (h)
1		89	100	18	97	100	12
2		63	100	30	48	100	18
3		86	100	30	77	100	26
4		50	100	18	52	100	16
5		95 <sup>c</sup>	91	30	99 <sup>c</sup>	89	22
6		24	100	30	26	100	18
7		15	100	23	20	100	13

<sup>a</sup> Reaction conditions: alkene (0.5 mmol), NaIO<sub>4</sub> (1 mmol), catalyst (600 mg), CH<sub>3</sub>CN/H<sub>2</sub>O (5/2.5 ml).<sup>b</sup> GC yield.<sup>c</sup> The by-product was 4-hydroxy-2-octene.

### 3.5. Alkene epoxidation with NaIO<sub>4</sub> in the presence of Mn(TMPyP)-NaX and Mn(TMPyP)-NaY under ultrasonic irradiation

The main effect of ultrasonic irradiation in liquids is a cavitation phenomenon, which is accompanied by a few extreme effects, such as a local increase in temperature, a local high pressure, the

**Scheme 2.** Proposed mechanism for oxidation of alkenes.




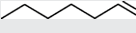


propagation of oxidation catalysts, and the formation of intense liquid microflows [48]. These effects may enhance liquid–solid mass transfer and cause physicochemical change in the processed medium considerably [49,50]. On the other hand, ultrasonic irradiation (US) can also be used to influence selectivity and yields of reactions. Therefore, all reactions were exposed to ultrasonic irradiation. The obtained results (Table 5) clearly showed that the reaction times reduced and the turnover frequencies (TOFs) increased in the systems under US irradiation.

In order to investigate the effect of ultrasonic irradiation, the size of catalysts were determined by particle size distribution technique before and after sonication. The results showed that the ultrasonic waves break-up the agglomerates. It seems that a part of ultrasonic irradiation effect is due to this phenomenon. On the other hand, ultrasonic irradiation increases the penetration of substrate to the zeolite cavities, and this lead to shorter reaction times as well as to higher product yields.

The two major mechanistic pathways for metal-catalyzed oxygen transfer are known to involve either peroxometal or oxometal species as the active intermediate. The peroxometal species are generally favored with early transition metals such as Mo(VI), W(VI) and V(V). On the other hand, many first row transition metals including manganese follow the metaloxo-catalyzed route.

These mechanistic processes observed in homogeneous complex catalysis may be applicable in the zeolite encapsulation metal

**Table 7**  
Epoxidation of linear alkenes with  $\text{NaIO}_4$  catalyzed by MnP-NaX and MnP-NaY under ultrasonic irradiation<sup>a</sup>.

Entry	Alkene	MnP-NaX			MnP-NaY		
		Conversion (%) <sup>b</sup>	Epoxide selectivity (%)	Time (h)	Conversion (%) <sup>b</sup>	Epoxide selectivity (%)	Time (h)
1		90	100	45	100	100	25
2		98	100	105	95	100	50
3		92	100	75	100	100	40
4		88 <sup>c</sup>	92	135	99 <sup>c</sup>	93	100
5		92	100	160	96	100	100
6		47	100	120	74	100	120

<sup>a</sup> Reaction conditions: alkene (0.5 mmol),  $\text{NaIO}_4$  (1 mmol), catalyst (600 mg),  $\text{CH}_3\text{CN}/\text{H}_2\text{O}$  (5/2.5 ml).

<sup>b</sup> GC yield.

<sup>c</sup> The by-product was 4-hydroxy-2-octene.

complexes [51]. For Mn(III)–zeolite encapsulated catalysts, the probable mechanism is shown in Scheme 2.

### 3.6. Shape selectivity in the epoxidation of linear alkenes

Epoxidation of linear alkenes with  $\text{NaIO}_4$  in the presence of MnP-NaX and MnP-NaY in aqueous acetonitrile at room temperature was also investigated (Tables 6 and 7). The results showed increasing the length of hydrocarbon chain led to lower epoxide yield and longer reaction times. It means that the structure of zeolites is sensitive to the chain length and shows a good selectivity towards linear alkenes. As the length of hydrocarbon chain increases the mobility of alkene decreases, and therefore, the accessibility of active site will be difficult. In the case of branched alkenes such as 4-methyl-2-pentene, the epoxide yield in both systems decreases, while 1-hexene with the same carbon atoms was epoxidized efficiently in both systems. One possible explanation is that the bulky methyl group at the 4-position does not allow the alkene to approach the active site because of strain spatial.

The results showed that MnP-NaX catalyst has higher catalytic activity in the epoxidation reactions and higher TOFs were obtained. This can be explained by the low amount of MnP loading in this catalyst when compared to the MnP-NaY one. Since when more cavities are occupied with a large amount of metalloporphyrin complex, the accessibility of alkene to the inner supercages decreases.

### 3.7. Catalyst recovery and reuse

The reusability of these catalysts was also investigated in the reaction of cyclooctene with  $\text{NaIO}_4$  under mechanical stirring and under ultrasonic irradiation. After each reaction the catalyst was filtered, washed consecutively with methanol and diethyl ether and reused in the next run. The results showed that this catalysts could be reused several times (two times was checked) without significant loss of their activity, but the reaction times increased. This may be due to the blocking of zeolite channels during the epoxidation reaction. The catalyst leaching was also investigated. The results showed that in the case of MnP-NaX no manganese was detected in the filtrates. But in the case of MnP-NaY only after the first run about 4% of Mn was leached from the zeolite.

## 4. Conclusion

MnP encapsulated into NaX and NaY zeolites obtained by the zeolite synthesis method was used as efficient and reusable catalysts in the alkene epoxidation with  $\text{NaIO}_4$ . In the epoxidation of linear alkenes with both catalytic systems a good shape selectivity was observed. Ultrasonic irradiation increased the catalytic

activity and higher product yield was obtained in shorter reaction times.

## Acknowledgement

The financial support of this work by Strategies Research Council of New Technologies of Isfahan Province (I.R. Iran) is acknowledged.

## References

- [1] B. Meunier, *J. Mol. Catal. A: Chem.* 113 (1996) 129.
- [2] A.E. Shilov, *J. Mol. Catal. A: Chem.* 47 (1988) 351.
- [3] B.R. Cook, T.J. Reinert, K.S. Suslick, *J. Am. Chem. Soc.* 108 (1986) 7281.
- [4] M.J. Nappa, C.A. Tolman, *Inorg. Chem.* 24 (1985) 4711.
- [5] Z. Gross, L. Simkhovich, *Tetrahedron Lett.* 39 (1998) 8171.
- [6] F.C. Skrobot, I.L.V. Rosa, A.P.A. Marques, P.R. Martins, J. Rocha, A.A. Valente, Y. Iamamoto, *J. Mol. Catal. A: Chem.* 237 (2005) 86.
- [7] O. Leal, D.L. Anderson, R.C. Bowman, F. Basolo, R.L. Burwell, *J. Am. Chem. Soc.* 97 (1975) 5125.
- [8] P.R. Cooke, J.R. Lindsay Smith, *J. Chem. Soc., Perkin Trans. 1* (1994) 1913.
- [9] K.J. Ciuffi, H.C. Sacco, J.C. Biazotto, O.A. Serra, O.R. Nascimento, E.A. Vidoto, C.A.P. Leite, Y. Iamamoto, *J. Non-Cryst. Solids* 273 (2000) 100.
- [10] F.S. Vinhado, P.R. Martins, A.P. Masson, D.G. Abreu, E.A. Vidoto, O.R. Nascimento, Y. Iamamoto, *J. Mol. Catal. A: Chem.* 188 (2002) 141.
- [11] M.D. Assis, J.R. Lindsay Smith, *J. Chem. Soc., Perkin Trans. 2* (1998) 2221.
- [12] I.L.V. Rosa, C.M.C.P. Manso, O.A. Serra, Y. Iamamoto, *J. Mol. Catal. A: Chem.* 160 (2000) 199.
- [13] D. Pattou, G. Labat, S. Defrance, J.L. Seris, B. Meunier, *New J. Chem.* 13 (1989) 801.
- [14] H.C. Sacco, Y. Iamamoto, J.R. Lindsay Smith, *J. Chem. Soc., Perkin Trans. 2* (2001) 181.
- [15] J.W. Huang, W.J. Mei, J. Liu, L.N. Ji, *J. Mol. Catal. A: Chem.* 170 (2001) 261.
- [16] E. Brulé, Y.R. de Miguel, *Tetrahedron Lett.* 43 (2002) 8555.
- [17] T.L. Poulos, in: K.M. Kadish, K.M. Smith, R. Guilard (Eds.), *The Porphyrin Handbook*, vol. 4, Academic Press, San Diego, 2000, p. 189.
- [18] P.J. O'Brien, *Chem. Biol. Interact.* 129 (2000) 113.
- [19] P.R. Ortiz de Montellano, *Cytochrome P450: Structure, Mechanism and Biochemistry*, Plenum, New York, 1995.
- [20] D.G. Kellner, S.C. Hung, K.E. Weiss, S.G. Sligar, *J. Biol. Chem.* 277 (2002) 9641.
- [21] S. Yoshioka, T. Toshi, S. Takahashi, K. Ishimori, H. Hori, I. Morishima, *J. Am. Chem. Soc.* 124 (2002) 14571.
- [22] A.D.Q. Ferreira, F.S. Vinhado, Y. Iamamoto, *J. Mol. Catal. A: Chem.* 243 (2006) 111.
- [23] A. Corma, *J. Catal.* 216 (2003) 298.
- [24] K.D. Karlin, *Science* 261 (1993) 701.
- [25] F. Bedioui, *Coord. Chem. Rev.* 144 (1995) 39.
- [26] I. Stiefel, in: J. Reedijk, E. Bouwman (Eds.), *Bioinorganic Catalysis*, Marcel Dekker, New York, 1999 (Chapter 3).
- [27] E.M. Serwicka, J. Połtowicz, K. Bahrnowski, Z. Olejniczak, W. Jones, *Appl. Catal. A: Gen.* 275 (2004).
- [28] B.Z. Zhan, X.Y. Li, *Chem. Commun.* (1998) 349.
- [29] T.A. Khan, J.A. Hriljac, *Inorg. Chim. Acta* 294 (1999) 179.
- [30] D.R. Corbin, N. Heron, *J. Mol. Catal.* 86 (1994) 343.
- [31] S.M. Csicsery, *Zeolites* 4 (1984) 202.
- [32] J. Turro, *Pure Appl. Chem.* 58 (1986) 1219.
- [33] R.F. Parton, G.J. Peere, P.E. Neys, P.A. Jacobs, R. Claessens, G.V. Baron, *J. Mol. Catal. A: Chem.* 135 (1998) 295.
- [34] J. Haber, K. Pamin, J. Połtowicz, *J. Mol. Catal. A: Chem.* 224 (2004) 153.
- [35] A.W. Van der Made, J.W.H. Smeets, R.J.M. Nolte, W. Drenth, *J. Chem. Soc., Chem. Commun.* (1983) 1204.

- [36] Y. Iamamoto, K.J. Ciuffi, H.C. Sacco, C.M.C. Prado, M. de Moraes, O.R. Nascimento, *J. Mol. Catal. A: Chem.* 88 (1994) 167.
- [37] F.S. Vinhado, C.M.C. Prado-Manso, H.C. Sacco, Y. Iamamoto, *J. Mol. Catal. A: Chem.* 174 (2001) 279.
- [38] P. Battioni, R. Iwanejko, D. Mansuy, T. Mlodnicka, J. Poltowicz, F. Sanchez, *J. Mol. Catal. A: Chem.* 109 (1996) 91.
- [39] K.J. Balkus Jr., A.G. Gabrielov, S.L. Bell, F. Bedioui, L. Roué, J. Devynck, *Inorg. Chem.* 34 (1994) 67.
- [40] G. Schulz-Ekloff, D. Wohrle, V. Iliev, E. Ignatzek, A. Andreev, in: H.G. Karge, J. Weitkamp (Eds.), *Zeolites as Catalysts, Sorbents and Detergents Builders*, Elsevier, Amsterdam, 1989, p. 315.
- [41] L. Barloy, J.P. Lallier, P. Battioni, D. Mansuy, Y. Piffard, M. Tournoux, J.B. Valim, W. Jones, *New J. Chem.* 16 (1992) 71.
- [42] K.O. Xavier, J. Chacko, K.K.M. Yussuff, *Appl. Catal. A: Gen.* 258 (2004) 251.
- [43] M.R. Maurya, A.K. Chandrakar, S. Chand, *J. Mol. Catal. A: Chem.* 263 (2007) 227.
- [44] A. Stone, E. Fleischer, *J. Am. Chem. Soc.* 11 (1968) 90.
- [45] D.W. Thomas, A.E. Martell, *J. Am. Chem. Soc.* 78 (1956).
- [46] S. Nakagaki, C.R. Xavier, A.J. Wosniak, A.S. Mangrich, F. Wypych, M.P. Cantao, I. Denicolo, L.T. Kubota, *Colloid Surf. A: Physicochem. Eng. Aspect* 168 (2000) 261.
- [47] M.L. Occelli, H.E. Robson, *Zeolite Synthesis*, American Chemical Society, Washington, DC, 1989.
- [48] M. Margulis, *Sonochemistry and Cavitation*, Gordon and Breach, New York, 1995.
- [49] M. Run, S. Wu, G. Wu, *Micropor. Mesopor. Mater.* 74 (2004) 37.
- [50] R. Ortiz de Montellano, *Cytochrome P-450, Structure, Mechanism and Biochemistry*, 2nd ed., Plenum Press, New York, 1995.
- [51] C. Linde, M.F. Anderlund, B. Akermark, *Tetrahedron Lett.* 46 (2005) 5597.